Kinetic Parameters Estimation of MgO-C Refractory by Shrinking Core Model

B.Hashemi[1)], *Z.A.Nemati*[2)†], *S.K.Sadrnezhaad*[2)] *and Z.A.Moghimi*[2)]
1) Department of Materials Science, School of Engineering, Shiraz University, Shiraz, Iran
2) Department of Materials Science and Engineering, Sharif University of Technology, Tehran 11365-9466, Iran
[Manuscript received July 8, 2005, in revised form March 6, 2006]

Kinetics of oxidation of MgO-C refractories was investigated by shrinking core modeling of the gas-solid reactions taking place during heating the porous materials to the high temperatures. Samples containing 4.5∼17 wt pct graphite were isothermally oxidized at 1000∼1350°C. Weight loss data was compared with predictions of the model. A mixed 2-stage mechanism comprised of pore diffusion plus boundary layer gas transfer was shown to generally control the oxidation rate. Pore diffusion was however more effective, especially at graphite contents lower than 10 wt pct under forced convection blowing of the air. Model calculations showed that effective gas diffusion coefficients were in the range of 0.08 to 0.55 cm^2/s. These values can be utilized to determine the corresponding tortuosity factors of 6.85 to 2.22. Activation energies related to the pore diffusion mechanism appeared to be around (46.4±2) kJ/mol. The estimated intermolecular diffusion coefficients were shown to be independent of the graphite content, when the percentage of the graphite exceeded a marginal value of 10.

KEY WORDS: Modeling; Kinetics; MgO-C; Oxidation; Diffusion coefficient

1. Introduction

Presence of graphite in MgO-C refractories results in good resistance to slag corrosion and thermal shock[1,2]. Direct and indirect oxidations of graphite degrade, however, these desirable effects. Direct oxidation results in lowering of the graphite content. Indirect reaction causes a major diminution in both magnesia and graphite percentage of the sample. Indirect oxidation (MgO+C=Mg+CO) is important at temperatures higher than 1400°C, while direct oxidation ($2C+O_2=2CO$) occurs at temperatures higher than 800°C. Both direct and indirect oxidation processes have, therefore, great influence on physical and chemical properties of the MgO-C refractories and need to be investigated in more details to determine their average life time[3∼5].

Presence of oxidizing atmosphere in steelmaking furnace causes graphite oxidation during oxygen lancing, metal tapping or waiting periods. Gas-solid reactions must, therefore, be considered in almost all stages of the steelmaking process[6∼8]. Numerous authors have written on kinetic modeling of gas-solid reactions[9∼13]. None of them provided, however, enough details on the oxidation kinetics of the MgO-C refractories. Faghihi-Sani and Yamaguchi[14], Ghosh *et al.*[15], Rongti *et al.*[16] and Li *et al.*[17] have, for example, studied the oxidation kinetics of MgO-C refractories. They did not, however, determine general model and prevailing mechanism of the process.

This paper follows last reports[18,19] and gives more details of achievement on MgO-C oxidation kinetics data and recent software developments related to gas-solid reactions occurring in a refractory type porous media. Samples containing different amounts of graphite (4.5∼17 wt pct) were isothermally oxidized at different temperatures and fractional weight losses were measured. Results were compared with the model predictions. Determination of the prevailing mechanisms resulted in determination of the effective diffusion coefficients and the involved activation energies.

Table 1 Particle size distribution of MgO

Size/mm	Percent/wt pct
3∼5	22.5
2∼3	14.2
0.1∼2	49.2
<0.1	14.1

2. Experimental

Cylindrical samples with 30 mm in diameter and 25 mm in height were prepared using Chinese sintered magnesia with a 9 wt pct MgO and natural graphite flakes with an ash content of 5 wt pct, which have been presented previously[18]. Particle size distributions of magnesia grains are shown in Table 1.

The samples contained 4.5∼17 wt pct graphite and 5 wt pct liquid phenolic resin (Novalac) as a binder. The samples were pressed uniaxially in a die press at pressures up to 120 MPa. The specimens were tempered at 240°C for 18 h prior to oxidation, heated at 600°C for 5 h in a coke bed to remove the volatile species. The bulk density and open porosity of samples were measured according to ASTM C20.

The samples were isothermally oxidized at 1000, 1175 and 1350°C, respectively for 3 h in a tubular furnace with 4.5 cm inside diameter, 45 cm height and a temperature accuracy of ±5°C as shown in Fig.1. Natural convection of air from bottom to top of the furnace provided the oxygen required for oxidation of the samples. A few samples were oxidized under blowing of the air from bottom of the furnace. Each sample was placed on an alumina tube that could be inserted, gradually, into the hot furnace at desired temperature in 2∼3 min and then weight loss was recorded *vs*

† Prof., Ph.D., to whom correspondence should be addressed, E-mail: nemati@sharif.edu.

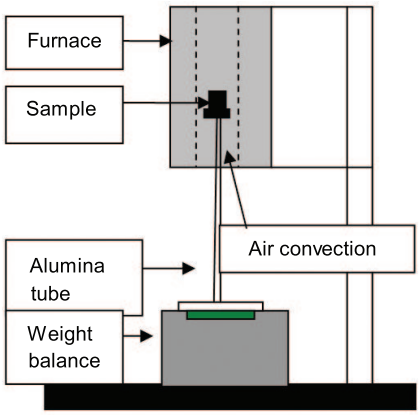

Fig.1 Schematic view of setup used for weight loss measurements

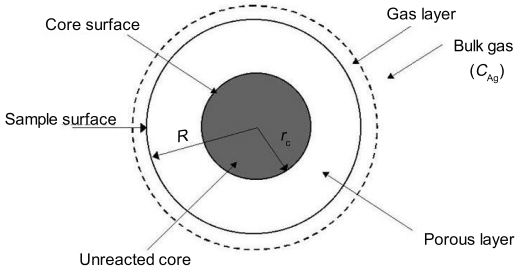

Fig.2 Cross-section of a cylindrical sample partially reacted with oxygen

time by an electronic balance with a weight accuracy of ±0.01 gr. To obtain a unidirectional process initiating from the sidewall and progressing towards the centerline of the sample, top and bottom of the samples were covered by alumina plates. To exactly determine total weight loss, from each group of samples having constant graphite content a typical, one was depicted and completely oxidized in a separate box furnace for a long time. The fractional weight loss (X) was then calculated from:

$$X = \frac{\text{Weight loss at time } t}{\text{Total weight loss after complete oxidation}}$$

3.Modeling

Shrinking core model with a first order isothermal gas-solid reaction occurring in a constant size specimen was used for development of the software[9]. The model depicted in Fig.2 assumes three steps comprising of mass transfer from gas layer or external diffusion (ext), gas diffusion inwards and outwards through the interstices of the specimens (dif) and chemical reaction at the unreacted core surface of the sample (che). A sharp boundary separates the non-oxidized zone from the oxidized region of the samples. Existence of the sharp reaction front indicates that chemical reaction is not the only controlling step in the system. The radius of the un-reacted core (r_c) is the main parameter in this model, which is related to the fractional weight loss (x) by x=1−(r_c/R)^2 (where R is the radius of the sample). According to the concept of additive reaction times and considering necessary corrections for sample bed diffusion and external mass transfer, the time t to achieve a certain degree of conversion x can be found as literature [9].

$$t = \tau_{che} \times f_{che}(x) + \tau_{dif} \times f_{dif}(x) + \tau_{ext} \times f_{ext}(x) \quad (1)$$

where t is overall reaction time; τ_{che}, τ_{dif} and τ_{ext} are time constants for chemical kinetics, diffusion and external mass transfer, respectively; $f_{che}(x)$, $f_{dif}(x)$ and $f_{ext}(x)$ are conversion functions describing kinetics, diffusion and mass transfer, respectively.

The conversion functions for different mechanisms are defined as follows:

$$f_{ext}(x) = x$$
$$f_{che}(x) = 1 - \sqrt{(1-x)}$$
$$f_{dif}(x) = x + (1-x) \times \ln(1-x)$$

For a specified controlling step, the overall reaction time is equal to multiplication of the corresponding time constant and conversion function. For double or three-mechanism systems, all corresponding terms should be considered to obtain the most appropriate result.

The conversion times are all positive quantities that can be obtained from the closest fit of the experimental data. Different methods can be used to find the best fit. Linear methods called "least square" and "least vertical distance" are both usable for this purpose. In a single-mechanism system, both methods are useable. For a limited number of empirical data, least vertical distance method gives more accurate result. Analytical solution of the "least square" relations is, however, usually easier than "least vertical distance" method. Although both methods are used to find the most appropriate relationship, the former has been applied to the systems with more than one controlling mechanism.

3.1 Single mechanism method

In single mechanism systems, experimental results ($x_i - t_i$) are simply translated into time *vs* $f_{che}(x)$, $f_{dif}(x)$ or $f_{ext}(x)$ plots. Those lines having minimum standard deviations from the experimental data demonstrate the dominant oxidation mechanism with the closest time constants τ_{che}, τ_{dif} or τ_{ext} being equal to slopes of the linear curves.

In the "least vertical distance" method, vertical distance of each point to the line of time *vs* $f_{che}(x)$, $f_{dif}(x)$ or $f_{ext}(x)$ is calculated. Sum of the vertical distances is minimized with selection of the best slope of the curve. The vertical distance between point A (t_i, $f(x_i)$) and the line of time *vs* $f_{che}(x)$, $f_{dif}(x)$ or $f_{ext}(x)$ is represented by the distance between points A and B (t_B, $f(x_B)$) shown in Fig.3. This distance d can be calculated from the following equation:

$$d^2 = (f(x_B) - f(x_i))^2 + (\tau \times f(x_B) - t_i)^2 \quad (2)$$

where $\tau = \frac{f(x_i) - f(x_B)}{t_B - t_i}$ and $f(x_B) = \frac{\tau \times t_i + f(x_i)}{1+\tau^2}$

Sum of the vertical distances is evaluated by:

$$\sum_{i=1}^{n} d_i^2 = \sum_{i=1}^{n} (f(x_B) - f(x_i))^2 + (\tau \times f(x_B) - t_i)^2 \quad (3)$$

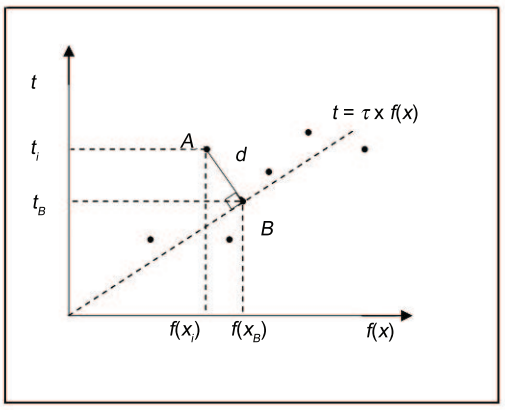

Fig.3 Vertical distance of the experimental results from line $t=\tau f(x)$

This quantity would be minimized when:

$$\frac{\partial}{\partial\tau}(\sum_{i=1}^{n}(f(x_B)-f(x_i))^2+(\tau\times f(x_B)-t_i)^2)=0 \quad (4)$$

Equation (4) has two roots. The positive root is only acceptable.

$$\frac{\partial}{\partial\tau}\Big(\sum_{i=1}^{n}\Big(\frac{\tau\times t_i+f(x_i)}{1+\tau^2}-f(x_i)\Big)^2+\Big(\tau\times\frac{\tau\times t_i+f(x_i)}{1+\tau^2}-t_i\Big)^2\Big)=0 \quad (5)$$

$$\tau=\frac{(-(\sum_{i=1}^{n}(f(x_i)^2-t_i^2))}{4\times(\sum_{i=1}^{n}(f(x_i)\times t_i))}+\frac{\sqrt{(\sum_{i=1}^{n}(f(x_i)^2-t_i^2))^2+4\times(\sum_{i=1}^{n}(f(x_i)\times t_i))^2)}}{4\times(\sum_{i=1}^{n}(f(x_i)\times t_i))}$$

3.2 Double mechanism systems

"Least square" method was used here. Standard deviation of the experimental results from the curve $t=\tau_{\rm che}\times f_{\rm che}(x)+\tau_{\rm dif}\times f_{\rm dif}(x)$ was calculated. Deviations summed up to be:

$$\sigma^2=\sum_{i=1}^{n}[t_i-\tau_1\times f_1(x_i)-\tau_2\times f_2(x_i)]^2 \quad (6)$$

Minimum deviation is obtained when:

$$\frac{\partial\sigma^2}{\partial\tau_1}=0 \quad (7)$$

$$\frac{\partial\sigma^2}{\partial\tau_2}=0 \quad (8)$$

Solving Eqs.(7) and (8) end up with the following relations:

$$\tau_1\times\sum_{i=1}^{n}f_1(x_i)^2+\tau_2\times\sum_{i=1}^{n}f_1(x_i)\times f_2(x_i)=\sum_{i=1}^{n}t_i\times f_1(x_i) \quad (9)$$

$$\tau_1\times\sum_{i=1}^{n}f_1(x_i)\times f_2(x_i)+\tau_2\times\sum_{i=1}^{n}f_2(x_i)^2=\sum_{i=1}^{n}t_i\times f_2(x_i) \quad (10)$$

Substituting for f_1 and f_2 results in the value of τ.

3.3 Triple mechanism systems

"Least square" technique was also used for assessment of the triple mechanism systems. Deviation of the experimental results from the line $t=\tau_{\rm che}\times f_{\rm che}(x)+\tau_{\rm dif}\times f_{\rm dif}(x)+\tau_{\rm ext}\times f_{\rm ext}(x)$ was evaluated and the summation of the deviations resulted in:

$$\sigma^2=\sum_{i=1}^{n}(t_i-\tau_{\rm che}\times f_{\rm che}(x_i)-\tau_{\rm dif}\times f_{\rm dif}(x_i)-\tau_{\rm ext}\times f_{\rm ext}(x_i))^2 \quad (11)$$

To minimize the total deviation, its derivatives must be zero:

$$\frac{\partial\sigma^2}{\partial\tau_1}=0,\quad \frac{\partial\sigma^2}{\partial\tau_2}=0,\quad \frac{\partial\sigma^2}{\partial\tau_3}=0$$

or:

$$\tau_{\rm che}\times\sum_{i=1}^{n}f_{\rm che}(x_i)^2+\tau_{\rm dif}\times\sum_{i=1}^{n}f_{\rm che}(x_i)\times f_{\rm dif}(x_i)+\tau_{\rm ext}\times\sum_{i=1}^{n}f_{\rm che}(x_i)\times f_{\rm ext}(x_i)=\sum_{i=1}^{n}t_i\times f_{\rm che}(x_i),$$

$$\tau_{\rm che}\times\sum_{i=1}^{n}f_{\rm che}(x_i)\times f_{\rm dif}(x_i)+\tau_{\rm dif}\times\sum_{i=1}^{n}f_{\rm dif}(x_i)^2+\tau_{\rm ext}\times\sum_{i=1}^{n}f_{\rm dif}(x_i)\times f_{\rm ext}(x_i)=\sum_{i=1}^{n}t_i\times f_{\rm dif}(x_i),$$

$$\tau_{\rm che}\times\sum_{i=1}^{n}f_{\rm che}(x_i)\times f_{\rm ext}(x_i)+\tau_{\rm dif}\times\sum_{i=1}^{n}f_{\rm dif}(x_i)\times f_{\rm ext}(x_i)+\tau_{\rm ext}\times\sum_{i=1}^{n}f_{\rm ext}(x_i)^2=\sum_{i=1}^{n}t_i\times f_{\rm ext}(x_i)$$

By solving the above equations, the values of $\tau_{\rm che}$, $\tau_{\rm dif}$ and $\tau_{\rm ext}$ are obtained.

4. Results and Discussion

Standard deviations of the experimental data from the straight time *vs* $f(x)$ lines were used to determine the controlling mechanism of the MgO-C oxidation system. Results (presented in Table 2) were consistent with the time constant data (Table 3). With a single-step presumption, the fractional weight loss measurements indicated a minimum standard deviation attributing to the gas mixture interdiffusion into the refractory pores. The best fit curves depicted for oxidation of the refractory samples containing 13 wt pct graphite at 1000 and 1350°C show a very small deviation tending to a negligible value as shown in Figs.4

Table 2 Standard deviation of oxidation results from the best fit line for different mechanisms

Sample	Graphite/wt pct	Temp./°C	Mechanism deviations/%				
			Che	Dif	Ext	Dif&Ext	Dif&Che
4G1	4.5	1350	13.91	1.43	23.45	1.13	1.12
4G2	4.5	1175	14.88	3.35	25.40	2.27	2.44
4G3	4.5	1000	18.00	1.98	22.93	–	–
9G1	9	1350	13.70	6.68	27.83	1.57	2.19
9G2	9	1175	16.70	5.96	26.15	2.05	2.21
9G3	9	1000	21.17	2.07	28.53	1.31	1.33
13G1	13	1350	14.40	5.38	25.04	1.48	1.74
13G2	13	1175	8.92	2.06	10.70	1.03	1.04
13G3	13	1000	15.70	3.26	20.44	0.73	0.72
17G1	17	1350	16.00	6.31	34.71	1.01	1.91
17G2	17	1175	23.10	7.56	37.48	1.46	1.60
17G3	17	1000	16.82	3.50	21.91	1.35	1.33

Table 3 Time constant of various mechanisms in one mechanism system

Sample	Mechanism		
	τ_{dif}/min	τ_{ext}/min	τ_{che}/min
4G1	177.93	118.65	161.80
4G2	194.02	128.66	175.79
4G3	328.67	145.22	229.58
9G1	224.90	155.50	206.44
9G2	322.95	177.77	262.83
9G3	418.44	192.82	301.258
13G1	239.99	150.69	211.27
13G2	457.67	128.30	221.95
13G3	485.40	186.70	304.89
17G1	255.28	180.57	234.186
17G2	412.45	241.50	384.94
17G3	497.60	192.40	313.70

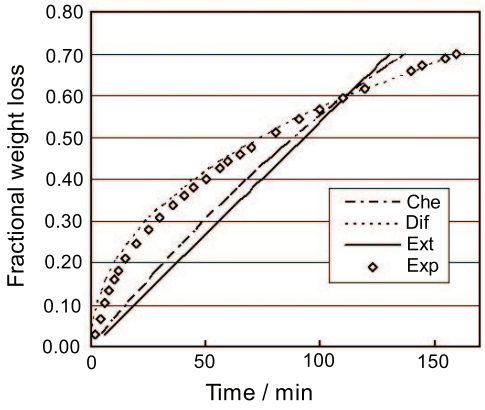

Fig.4 Experimental and software evaluations of the fractional weight loss for samples containing 13 wt pct graphite at 1000°C

and 5. Assuming a double step mechanism, the lowest standard deviations were associated with pore diffusion process combined with an external boundary layer gas transfer. Above 1000°C, the chemical reaction is usually too fast to be considered as a controlling stage. The best-fit plots shown in Fig.6 indicate the smallest possible differences between the experimental and calculated data. External layer gas transfer step does not appear to show any considerable effect unless a double mechanism system is taken into account. Time constant of the oxidized samples is shown in Table 4. These data are obtained at 1250°C for different air flow rates. It is seen that τ_{ext} de-

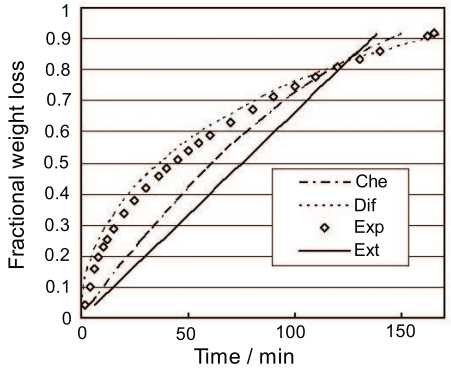

Fig.5 Experimental and software evaluations of the fractional weight loss for samples containing 13 wt pct graphite at 1350°C

creases with increasing air flow rate. Similar data are plotted in Fig.7 for internal diffusion mechanism. As air flow increases, deviation from straight line of the experimental data becomes lower. At 50 SCFH (standard cubic foot per hour) the best straight line fit is obtained.

The diffusional time constant (τ_{dif}) of different samples are shown in Table 5. They are calculated based on a double mechanism process. Effective coefficient of gas diffusion (D_e) was calculated from the time constant evaluated from the best fitting curves:

$$\tau_{dif} = (\rho_m R^2)/(8c_{O_2} D_e)^{[12]} \quad (12)$$

where ρ_m is molar density of graphite in the sample, R is initial radius of the sample, c_{O_2} is bulk concentration of oxygen at the exterior of the sample and D_e is the effective diffusion coefficient of the gas phase. Figure 8 shows that the effective diffusion coefficient increases with the graphite content of the sample. With increasing the graphite content, the volumes associated with the graphite flakes increase as well. Higher amounts of pores are then produced as a result of the oxidation progress. With an extremely porous layer, the inter-diffusivity of O_2 and CO is much larger within the macropores created in the oxidized layer.

Variation of the effective diffusion coefficient of the samples containing 9 wt pct graphite is plotted against temperature in Fig.9. Linear relation of $\ln(D_e)$ with $(1/T)$ is due to exponential relation between them. The slope of the line is proportional to

Table 4 Time constant of the samples oxidized at 1250°C with air

Sample	Temp./°C	Density/(g/cm^3)	Graphite/(%)	Air flow/SCFH	τ_{dif}/min	τ_{ext}/min
GC1	1250	2.50	16.4	0	153.04	15.16
GC2	1250	2.49	16.4	30	135.94	9.89
GR1	1250	2.77	20.2	0	333.31	24.03
GR2	1250	2.77	20.1	25	293.96	6.64
GR3	1250	2.78	20.1	50	281.00	1.30
G1	1175	2.67	21.2	0	300.10	55.37
G2	1175	2.67	21.2	25	259.80	44.57

Table 5 Diffusion controlled time constant, initial porosity and graphite molar density of the different samples

Sample	Temp./°C	Molar density of graphite	τ_{dif}/min	Porosity/%
4G1	1350	0.0108	167.2	13.5
4G2	1175	0.0108	200.4	13.6
4G3	1000	0.0108	328.4	13.4
9G1	1350	0.0207	182.3	11.9
9G2	1175	0.0207	265.7	11.9
9G3	1000	0.0207	396.1	11.8
9G4	900	0.0206	461.7	12.0
13G1	1350	0.0293	198.8	11.5
13G2	1175	0.0295	287.2	11.4
13G3	1000	0.0294	420.0	11.4
17G1	1350	0.0371	213.0	11.3
17G2	1175	0.0372	304.1	11.5
17G3	1000	0.0371	433.0	11.3

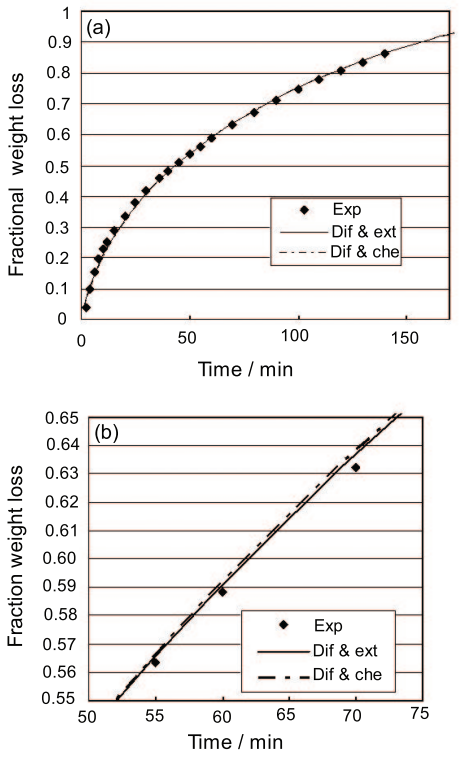

Fig.6 (a) Comparison of the experimental and software results of double mechanism system for sample initially containing 13 wt pct graphite oxidized at 1350°C, (b) enlarged part of Fig.6(a)

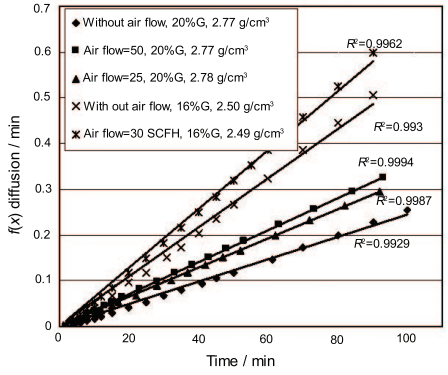

Fig.7 Diffusion mechanism function of the samples oxidized at 1250°C, where G presents graphite

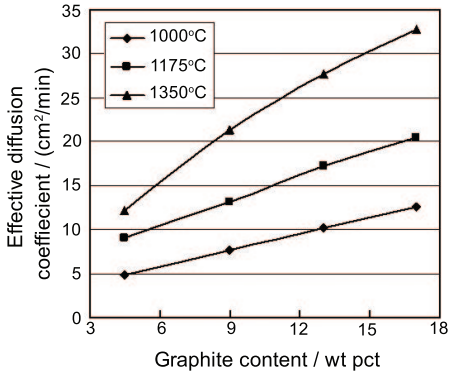

Fig.8 Effective diffusion coefficient *vs* initial graphite content of the samples

the activation energy for diffusion. The activation energy for gas diffusion in the samples is averaged to about (46.4±2) kJ/mol.

Inter diffusion of the gases within the pores consists of concomitant inward O_2 *vs* outward CO transfer through the oxidized porous layer. This process can occur by one, two or any combination of three mechanisms called molecular, Knudsen or surface

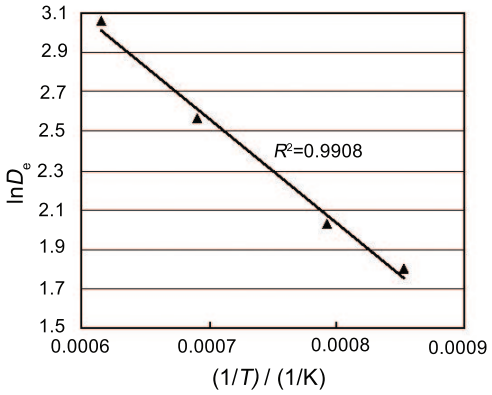

Fig.9 Variation of $\ln(D_e)$ *vs* temperature for samples containing 9 wt pct graphite

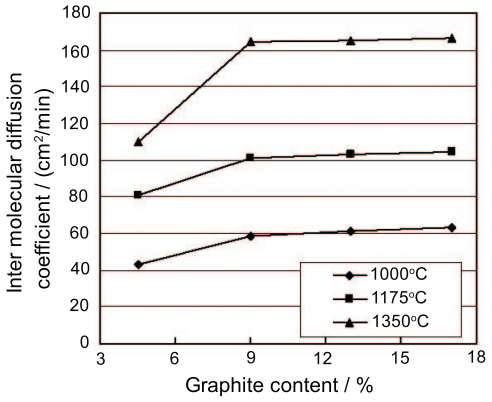

Fig.10 Inter-diffusion coefficient *vs* graphite content of the samples

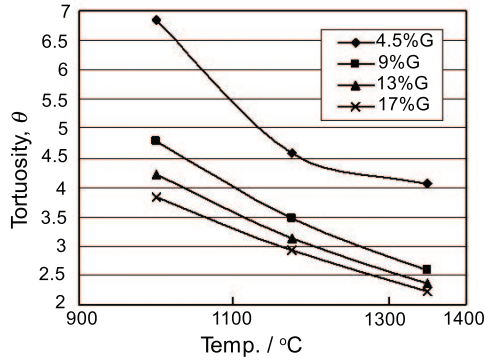

Fig.11 Variation of tortuosity *vs* temperature of samples with different graphite content

diffusion, respectively. The share of each stage depends on the pore′s structure and volume of the oxidized layer. From literature [12], the effective diffusion coefficient is defined as:

$$D_e = D_{O_2-CO}\frac{\varepsilon}{\theta} \tag{13}$$

where D_{O_2-CO} is the molecular diffusivity of O_2 in CO, ε is the total porosity content of the oxidized layer and θ is tortuosity of the pores. Since determination of θ, is not too easy, it is approximated by the term $\varepsilon^{-1/2}$[12]. The total porosity content of the oxidized layer is calculated based on the initial porosity and the initial graphite content of the sample. Substituting the values of ε and D_e into Eq.(13), one can obtain the amount of the inter-diffusion coefficient (D_{O_2-CO}). Figure 10 shows the variation of D_{O_2-CO} *vs* graphite content of the samples. Within the experimental ranges of temperature and porosity, the values of D_{O_2-CO} are nearly independent of the graphite content, when graphite content is greater than 9 wt pct. Szekely *et al.*[20] has previously indicated that at high sizes of the pores, the gaseous diffusion is dominated by molecular diffusion and is, therefore, independent of the pore size. Our findings show that at high graphite contents, due to the increase in the size of the pores at oxidized layer, the gas diffusion coefficient is independent of the pore size of the samples. Lower values of the molecular diffusion coefficient for samples containing 4.5 wt pct graphite may be due to the lower total porosity of the samples and deviation from pure molecular diffusion mechanism to a mixed one.

To evaluate the effects of temperature and the graphite content of the sample on the tortuosity (θ) of the pores, Eq.(13) was used with the quantities of the molecular diffusion coefficient (D_{O_2-CO}), the effective gas diffusion coefficient (D_e) and the porosity content ε determined at different temperatures and graphite contents. Chapman-Enskog equation[20] was used to determine D_{O_2-CO}; time constant was used to determine D_e and the initial porosity and graphite content of the sample was used to determine ε. Variation of tortuosity with temperature and initial graphite content of the samples is shown in Fig.11. It is seen that the amount of tortuosity decreases with increasing the temperature and the initial graphite content. The decrease in the tortuosity with increasing the initial graphite content can be attributed to the enlargement of the holes produced within the porous layer of the MgO-C refractory because of the oxidation reactions. By increase in the temperature, the shape of the holes may also change due to both localized heating and sintering processes that may occur owing to the much faster oxidation reactions.

5. Conclusions

(1) A computer program was developed to predict the oxidation mechanisms of the MgO-C refractories at high temperatures under normal atmosphere. The software showed capability of extracting kinetic parameters from the empirical information.

(2) Pore diffusion is the predominant mechanism that controls the oxidation rate of the high graphite content refractory samples.

(3) By the diffusion time constant, obtained from the model, the effective diffusion coefficient was determined.

(4) Variations of the tortuosity factor of the pores were determined against temperature and graphite content by using semi-empirical data and the simulated kinetic results.

REFERENCES

[1] A.Yamaguchi, S.Zhang and S.Hashimoto: in Proceedings of Unified International Technical Conf. on *Re-*

fractories, Tokyo, Japan, 1995, 341-348.
[2] S.Banerjee: in Proceedings of International Technical Conf. on *Refractories,* Alfaro, Mexico, 2001, 1033-1041.
[3] A.Watanabe, H.Takahashi and F.Nakatani: *J. Am. Ceram. Soc.,* 1986, **69**(9), c-213.
[4] B.Baker and B.Brezny: in Proceedings of International Technical Conf. on *Refractories,* Aachen, Germany, 1991, 168-172.
[5] A.Yamaguchi: *Taikabutsu Overseas,* 1984, **4**(1), 32.
[6] M.Rigaud, C.Richmond and P.Bombard: *Proceedings of Unitecr 91,* Aachen, Germany, 1991, 266.
[7] V.L.Lou, T.E.Mitchell and A.H.Heuer: *J. Am. Ceram. Soc.,* 1985, **68**(2), 49.
[8] A.Yamaguchi: *Taikabutsu Overseas,* 1987, **7**(1), 4.
[9] N.Mazet and B.Spinner: *Int. Chem. Eng.,* 1992, **32**(2), 271.
[10] N.Mazet and B.Spinner: *Int. Chem. Eng.,* 1992, **32**(2), 395.
[11] S.K.Sadrnezhaad, A.Gharavi and A.Namazi: *IJE Trans. A: Basics,* 2003, **16**(1), 61.
[12] R.W.Missen and C.A.Mims: *Introduction to Chemical Reaction Engineering and Kinetics,* John Wiley and Sons, New York, 1999, 224.
[13] O.Levenspiel: *Chemical Reaction Engineering,* John Wiley and Sons, New York, 1972, 357.
[14] M.A.Faghihi-Sani and A.Yamaguchi: *Ceram. Int.,* 2002, **28,** 835.
[15] N.K.Ghosh, D.N.Ghosh and K.P.Jagannathan: *Brit. Ceram. T.,* 2000, **99**(3), 124.
[16] L.Rontgi, P.Wei, M.Sano and J.Li: *Thermochim. Acta,* 2002, **390,** 145.
[17] X.Li, M.Rigaud and S.Palco: *J. Am. Ceram. Soc.,* 1995, **78**(4), 965.
[18] B.Hashemi, Z.A.Nemati and S.K.Sadrnezhaad: *China′s Refractories,* 2004, **13**(2), 13.
[19] B.Hashemi, Z.Moghimi, Z.A.Nemati and S.K.Sadrnezhaad: 4th Inter. Symp. on *Advances in Refractories for the Metallurgical Industries,* Hamilton, Ontario, Canada, 2004, 581.
[20] J.Szekely, J.W.Evans and H.Y.Sohn: *Gas-Solid Reactions,* Academic Press, New York, 1976, 8.